HHS Public Access

Author manuscript

Nat Genet. Author manuscript; available in PMC 2013 January 01.

Published in final edited form as:

Nat Genet. ; 44(7): 788–792. doi:10.1038/ng.2275.

Mutations in the PCNA-binding domain of *CDKN1C* cause IMAGE Syndrome

Valerie A. Arboleda[1], **Hane Lee**[1,2], **Rahul Parnaik**[3], **Alice Fleming**[1], **Abhik Banerjee**[1], **Bruno Ferraz-de-Souza**[3,4], **Emmanuèle C. Délot**[5], **Imilce A. Rodriguez-Fernandez**[1], **Debora Braslavsky**[6], **Ignacio Bergadá**[6], **Esteban C. Dell'Angelica**[1], **Stanley F. Nelson**[1,2], **Julian A. Martinez-Agosto**[1,5], **John C. Achermann**[3], and **Eric Vilain**[1,5,7]

[1]Department of Human Genetics, David Geffen School of Medicine, University of California, Los Angeles

[2]Department of Pathology, David Geffen School of Medicine, University of California, Los Angeles

[3]Developmental Endocrinology Research Group, Clinical & Molecular Genetics Unit, University College London, Institute of Child Health, London UK

[4]Department of Endocrinology/LIM-18, University of Sao Paulo School of Medicine, Sao Paulo, Brazil

[5]Department of Pediatrics, David Geffen School of Medicine, University of California, Los Angeles

[6]Division of Endocrinology, Hospital de Niños "Ricardo Gutierrez", Buenos Aires, Argentina

[7]Department of Urology, David Geffen School of Medicine, University of California, Los Angeles

Introductory

IMAGE Syndrome (Intrauterine growth restriction, Metaphyseal dysplasia, Adrenal hypoplasia congenita, and Genital anomalies) is an undergrowth developmental disorder with life-threatening consequences[1]. Identity-by-descent analysis in a family with IMAGE syndrome[2] identified a 17.2 megabase (Mb) locus on 11p15 that segregated in affected family members. Targeted exon array capture of the disease locus, followed by high-throughput genomic sequencing and validated by dideoxysequencing, identified missense mutations in imprinted gene *CDKN1C (P57KIP2)* in two familial and four unrelated

Correspondence should be addressed to Eric Vilain (evilain@ucla.edu).

Author Contributions. V.A.A. designed and performed the experiments, analyzed data, and wrote the paper. E.V. designed the project, supervised the overall experiments, and wrote the paper with V.A.A. H.L. and S.F.N. contributed to design and analysis of the linkage and sequencing data. Em.C.D. contributed to the design of cell-cycle analysis experiments and editing of the manuscript. A.F., Es.C.D. and I.R.F. contributed to the nuclear localization experiments and design of the PCNA and ubiquitin assays. D.B. and I.B. clinically assessed and extracted DNA from Family A. R.P., B.F.-d.S., and J.C.A. performed immunofluorescence and RT-PCR experiments. A.B. and J.A.MA. performed, analyzed, and contributed to the writing of the *Drosophila* experiments. All authors discussed the results and implications of the work and commented on the manuscript at various stages.

Competing financial interests

The authors declare no competing financial interests.

URLs. http://www.novocraft.com/index.html, http://bfast.sourceforge.net, http://picard.sourceforge.net/, http://samtools.sourceforge.net/, http://genome.ucsc.edu, http://seqware.sourceforge.net

patients. Familial analysis demonstrated an imprinted mode of inheritance where only maternal transmission of the mutation resulted in IMAGE syndrome. *CDKN1C* inhibits cell-cycle progression[3] and targeted expression of IMAGE-associated *CDKN1C* mutations in *Drosophila* caused severe eye growth defects compared to wild type *CDKN1C*, suggesting a gain-of-function mechanism. All IMAGE-associated mutations clustered in the PCNA-binding domain of *CDKN1C* and resulted in loss of PCNA binding, distinguishing them from *CDKN1C* mutations that cause Beckwith-Wiedemann Syndrome, an overgrowth syndrome[4].

Since the initial description of IMAGE syndrome (OMIM #300290)[1], a number of isolated and familial cases have been reported[1,5–11]. In order to identify a causative gene for IMAGE syndrome, we performed a 250K *Nsp* Affymetrix SNP Array on seven affected and one unaffected sibling from Family A, a five-generation family from Argentina (Fig. 1a). Further analysis using a custom script detected a 17.2 Mb identical-by-descent (IBD) region on chromosome 11, shared by seven affected family members but not an unaffected sibling (Fig. 1b), with a LOD score of 5.4. Despite the multisystem involvement of IMAGE syndrome, we did not identify a contiguous gene deletion or duplication in the affected individuals (Supplementary Fig. 1).

To determine the causative mutation, we performed targeted high-throughput genomic sequencing of all the exons within a conservative IBD region. An Agilent 244K custom CGH array was designed to capture all exons and splice sites within the region spanning 0–22.6 Mb on chromosome 11. In total, five custom bar-coded genomic DNA libraries (Family A, V-1 and V-6; unrelated Patients 1, 2, and 3) were prepared, pooled, and captured on a single custom array, and the DNA enriched for the IBD region was sequenced on one lane of the Illumina Genome Analyzer II. Our targeted approach yielded an average coverage of 32x. Patient 3 had a significantly lower coverage of 9x across the targeted intervals and was not used in the initial bioinformatics analysis. In the remaining four samples analyzed, ~85% of all targeted regions were covered at ≥10x.

The pedigree and IBD analysis led us to hypothesize that IMAGE syndrome was inherited as a rare autosomal dominant disorder. Our bioinformatics analysis required that both V-1 and V-6 share the same rare gene variant, and at least one of the non-related IMAGE syndrome patients harbor a rare variant (defined as a variant not present in dbSNP129) in the same gene. This approach identified a single gene, *CDKN1C.*

Upon further examination, we noted that *CDKN1C* was captured and sequenced at a much lower rate compared to other targeted genes due to a high GC-content of ≥80%. To compound this low gene coverage, we re-sequenced *CDKN1C* by dideoxysequencing (primers listed in Supplementary Table 1) in all five individuals sequenced by high-throughput sequencing and in an additional sporadic case (Patient 4). Affected individuals from Family A carried a c.825T>G change resulting in a F276V missense mutation. The four unrelated patients with IMAGE syndrome harbored four mutations in *CDKN1C*: F276S, R279P, D274N, and K278E (Table 1). In total, we identified five rare heterozygous missense mutations in *CDKN1C* that cluster within six amino acids of the PCNA-binding domain[12] (Fig. 2a). All variants localized to a highly conserved region[13] (Fig. 2b) and are

predicted to be “damaging” to the structure and function of *CDKN1C* by Polyphen analysis[14].

CDKN1C is located on chromosome 11 and encodes a protein known to play a key role in inhibiting cell cycle progression. In most tissues, the paternal allele is repressed by distant imprinting control regions, such that expression is primarily from the maternal allele[15,16]. Inheritance of IMAGE syndrome in Family A was only through maternal transmission of the *CDKN1C* mutation (Fig. 1a). Sequencing for the c.825T>G mutation in 24 members from Family A confirmed that only individuals who inherited the mutation on the maternal allele are affected. A c.825T>G mutation inherited on the paternal allele was not expressed, presumably because of epigenetic silencing of the mutated allele.

To confirm the pathogenicity of these mutations, we used an *in vivo* functional model in which IMAGE-associated human *CDKN1C* mutants were expressed in *Drosophila melanogaster* using the GAL4 UAS system[17]. Ubiquitous overexpression of wild type or mutant *CDKN1C* resulted in early larval lethality. Targeted expression of the IMAGE-associated *CDKN1C* mutants resulted in altered wing vein patterning and decreased wing size (see Supplementary Fig. 2 & 3). Expression of wild type *CDKN1C* restricted to the eye did not have any effects on adult eye size, while expression of IMAGE-associated *CDKN1C* mutants showed a moderate to severe reduction in eye size (Fig. 3).

Overexpression of IMAGE-associated *CDKN1C* mutants in HEK293T cells did not interfere with the ability of CDKN1C to inhibit the cell cycle in G0/G1 through binding of the CDK-domain (Supplementary Fig. 4). These data suggest that IMAGE-mutations within the PCNA-binding domain do not inhibit cell-cycle progression and likely act through a different mechanism resulting in IMAGE syndrome.

CDKN1C is located within an imprinted cluster of genes that regulate prenatal and postnatal growth and development. Genetic alterations in *CDKN1C* have been shown to give rise to Beckwith-Wiedemann Syndrome (BWS; OMIM #130650), an overgrowth disorder[18,19] Here, we show that an undergrowth condition, IMAGE syndrome, is caused by domain-specific mutations in the maternally inherited allele of *CDKN1C*.

Both BWS human patients and *CDKN1C*$^{-/-}$ knockout mice exhibit adrenal hyperplasia[20,21] in contrast to the adrenal hypoplasia in IMAGE patients. We therefore verified that *CDKN1C* mRNA and protein are expressed in the developing human adrenal gland (Fig. 4). Quantitative RT-PCR demonstrated that the expression of *CDKN1C* is greater in adrenal tissue during early human development than in brain or muscle (Fig. 4a). Immunohistochemistry showed strongest expression of *CDKN1C* within a subset of cells in the subcapsular or developing definitive zone of the adrenal gland (Fig. 4b).

To determine if BWS and IMAGE mutations work through the same mechanism, we repeated the above functional studies with BWS-specific mutants. In the cell cycle analysis, transfection of the BWS-mutant *CDKN1C-L42P* resulted in a loss of cell cycle inhibition at G0/G1. Ubiquitous expression of BWS-associated *CDKN1C* mutations in *Drosophila melanogaster* were early larval lethal, however targeted expression had no effect on eye size, wing size, or wing vein patterning (Fig. 3g,h, Supplementary Fig. 2e,2f,3e,3f). Thus, *in*

vitro and *in vivo*, BWS mutants have different effects relative to the IMAGE mutants suggesting that domain-specific mutations have differential effects on cell cycle progression and developmental processes.

BWS-associated *CDKN1C* mutations are either missense mutations localized to the cyclin-dependent kinase binding domain or nonsense mutations, both of which result in protein loss-of-function, over proliferation, and predisposition to cancer[22] due to loss of cell-cycle inhibition[3]. In contrast, we show that missense mutations localized to a highly conserved region of the PCNA-binding domain of *CDKN1C* in IMAGE syndrome resulted in excess inhibition of growth and differentiation—a gain of function (Fig. 5).

Since two of the five mutations fall into a putative nuclear localization signal, we determined whether IMAGE mutants interfere with active nuclear transport of CDKN1C. H295R and M1 cells transfected with GFP-CDKN1C fusion constructs (Supplementary Fig. 5), showed that none of the tested IMAGE mutants interfered with active transport mechanisms or with binding affinity to α-importin.

Since IMAGE mutations cluster in a domain known to bind PCNA, we performed co-immunoprecipitation experiments to test the effect of IMAGE mutations on PCNA binding. HEK293T cells were transfected with flag-tagged CDKN1C constructs bearing the wild type or IMAGE alleles (F276V and K278E). Endogenous PCNA was recovered from the wild type but not IMAGE immunoprecipitates (Fig. 4c), suggesting that PCNA binding is disrupted in mutants.

Since one of the roles of *PCNA* is to facilitate ubiquitination of cell cycle proteins[23], we investigated the role of IMAGE mutations in PCNA-dependent ubiquitination of CDKN1C. HEK293T cells were co-transfected with flag-tagged wild type or IMAGE-mutant F276V CDKN1C and with HA-tagged Ubiquitin (12 kDa) and subjected to co-immunoprecipitation. CDKN1C migrates at ~50 kDa, and therefore we expect the mono-, di-, and poly-ubiquitinated CDKN1C to migrate at ~62 kDa or higher depending on the number and the branching of the ubiquitin moieties. Here we show that a band at 63 kDa, the approximate size of a monoubiquitinated CDKN1C protein, is present in the wild type CDKN1C but absent in the IMAGE mutant sample (Fig.4d).

Our data reveal a role for PCNA binding in a specific ubiquitination modification of *CDKN1C*. Many cell cycle proteins are subject to PCNA-dependent ubiquitination[24], which has pleiotropic effects. Monoubiquitination, as observed in our data, may have a number of functional consequences, such as modulation of protein localization, of protein interactions, and of proteosomal degradation[25,26,27]. The latter is less likely because it typically requires, at minimum, tetra-ubiquitination[28], but cannot be ruled out without information on CDKN1C protein stability.

Next generation sequencing has emerged as a powerful tool in identifying rare Mendelian disease genes, utilizing existing linkage analysis data to identify a disease gene in an unbiased fashion. Our findings show that missense mutations in the PCNA-binding domain have an inhibitory effect on growth, via loss of binding of PCNA to CDKN1C, thereby altering ubiquitination of CDKN1C and presumably promoting its function. The contrast

between BWS and IMAGE mutations in *CDKN1C* highlights the dual and opposing effects of specific *CDKN1C* mutations. Mutations within the PCNA-binding site of *CDKN1C* blocked *in vivo* growth and differentiation and may illuminate novel mechanisms regulating cell transformation[12], tumor growth, and cell cycle progression.

METHODS

Study Subjects

All participants were patients diagnosed clinically with IMAGE syndrome. This study was approved by the Institutional Review Board (IRB) at the University of California, Los Angeles, the Hospital de Niños Ricardo Gutierrez in Argentina, or the Institute of Child Health at University College London. All participants provided informed consent. Phenotypes are summarized in Table 1.

Identity-by-descent analysis

Genomic DNA from 7 affected individuals (IV-10, V-1, V-2, V-5, V6, V-7, V-12) and 1 non-affected individual (V-13) from a large Argentine family (Family A) were genotyped on the Affymetrix 250K *Nsp1* SNP arrays, as per manufacturers' protocol. Familial relationships were confirmed through checking the sharing statistics in all pairs of samples and ancestral identity-by-descent (IBD) analysis was performed using a custom script (B. Merriman, available on request). The IBD analysis script was designed to search for long continuous intervals compatible with a common extended haplotype among all the affected individuals but not with the unaffected individuals.[29] A conservative error rate of 1% was used to allow the algorithm to tolerate possible genotyping errors. A rare dominant model of inheritance was assumed with rare frequency of this haplotype of 0.1% and penetrance of 100% under the assumption that the carriers (parents of the affected individuals) were not showing the phenotype for a different reason (i.e. imprinting) than low penetrance of the disease phenotype.

Capture and Sequencing of Genomic DNA

For the capture of the genes within the IBD interval, we used Agilent Custom 244K comparative genomic hybridization Array. The 60-bp oligonucleotide probes were tiled every 20-bp against all exonic regions on chromosome 11 between 2.45-20.15Mb (hg18, March 2006, build 36.1) and every 30-bp in the flanking 5' and 3' regions spanning 0-2.45 Mb and 20.15-22.6 Mb. We included all gene models identified in RefSeq, Genbank, CCDS and UniProt. Location and sequence of all probes are available upon request.

Genomic DNA libraries were created for patients V-1 an V-6 from Family A and 3 isolated cases of IMAGE[1] (Patient1, 2, and 3) following manufacturer's protocol (Illumina protocol Preparing Samples for Sequencing Genomic DNA, p/n 11251892 Rev. A) except for the adaptor ligation step where we used custom-made, internally validated bar-coded adaptors. After the PCR amplification, five bar-coded libraries were pooled together and captured by hybridization to custom-designed CGH array, as described in [30]. After the capture, the array was washed and the captured DNA was eluted, amplified and diluted to 10nM final concentration based on the Qubit concentration measure and Agilent Bioanalyzer. One

flowcell lane of single-end sequencing was performed at the UCLA Genomic Sequencing Center on the Illumina Genome Analyzer II for 76x cycles following manufacturer's protocol. The base-calling was performed by the real time analysis software (Illumina).

Sequence Data Analysis

The Illumina output files (.qseq) were converted to fastq formats using BFAST[31,32] script ill2fastq.pl and then parsed into multiple fastq files, each for one unique barcode. Only the reads with 100% matching barcode sequences were carried over to the second set of fastq files. The sequence reads in each fastq file were aligned to the human reference genome (hg18, March 2006, build 36.1) using Novoalign from Novocraft Short Read Alignment Package. The output format was set to SAM and default settings were used for all options. Using SAMtools, the SAM file of each sample was converted to a BAM file, sorted and merged and potential PCR duplicates were removed using Picard[33]. The variants, both single nucleotide variants (SNVs) and small INDELs (insertions and deletions), within the captured coding exonic intervals were called using the SAMtools pileup tool. For SNV calling, the last 5 bases were trimmed and only the reads lacking INDELs were retained. For INDEL calling, only the reads that contained one contiguous INDEL, not occurring on either end of the read, were retained[34]. The variants were further annotated using the SeqWare project and loaded into the SeqWare QueryEngine database[35]. Variants from each sample with the following criteria were identified: (i) variant base or INDEL observed at least twice and at ≥5% of the total coverage per base, (ii) variant observed at least once on both forward and reverse strands, (iii) SNV quality score ≥10. As IMAGE syndrome is a rare condition, only variants with coding consequences not present in dbSNP129 were further analyzed.

CDKN1C Sequencing

All *CDKN1C* (RefSeq: NM_000076.2) mutations were PCRed using Phusion HF polymerase (NEB) with 5% DMSO and 0.1M Betaine. PCR products were sent for dideoxysequencing at Laragen, Inc. PCR primers used are listed in Supplementary Table 1. All mutation locations were reported using CCDS7738.1 and P49918 as the normal transcript and protein sequences, respectively.

Plasmid Constructs

The cDNA of CDKN1C cloned into pBluescript was purchased from ATCC(#99411)[36]. Mutations were generated using site-directed mutagenesis (Stratagene, primers in Supplementary Table 1). 4 mutants were created, corresponding to BWS mutations (p.L42P and c.826delT) and IMAGE syndrome mutations (p.F276V and p.K278E). Wild type and mutant versions of *CDKN1C* were subcloned into pCDNA3.1(+) and pEGFP-C2 for mammalian cell culture experiments, into pFLAG-pcDNA3.1 for the immunoprecipitation, and into pUAST for the generation of transgenic flies.

Quantitative Reverse Transcription PCR

Human tissue from 7–8 weeks post-conception (wpc) was provided by the Medical Research Council/Wellcome Trust-funded Human Developmental Biology Resource with Research Ethics Committee approval and informed consent. RNA was extracted from adrenal, brain

and muscle samples using the TRIzol reagent and first-strand cDNA was generated using SuperScriptR II reverse transcriptase (Invitrogen). Expression of *CDKN1C* transcript was assessed by quantitative PCR using the StepOnePlus Real-time PCR System, TaqManR Gene Expression Assays for human *CDKN1C* (Hs00175938_m1) and human *GAPDH* as endogenous control (4333764T; all Applied Biosystems). Data were analyzed with StepOne software v2.1 according to the $2^{-\Delta\Delta CT}$ method.

Immunofluorescence

Fourteen-micron sections of human fetal adrenal tissue (8 weeks post conception) were fixed briefly in 4% PFA and blocked in 1% BSA before incubating overnight with antibody to CDKN1C (Fisher AFMA121866) and CYP11A1 (Sigma HPA016436). Primary antibodies were detected using Alexa647 goat anti-mouse (Invitrogen, A21235) and Alexa555 (Invitrogen, A21429) goat anti-rabbit conjugates. Nuclei were counterstained with DAPI. IMAGEs were collected on a Zeiss 710 confocal microscope (Carl Zeiss).

Immunoprecipitation

HEK293T cells were transfected with constructs encoding Flag-CDKN1C with Lipofectamine 2000 (Invitrogen). For ubiquitination assays, cells were co-transfected with pCI-neo-$(HA)_3$-human Ub[37] construct and treated 3 hours in 10μM MG-132 (Millipore) prior to cell lysis. Flag-CDKN1C was immunoprecipitated from cell lysates using the ANTI-FLAG M2-Agarose Affinity Gel (Sigma-Aldrich). Western blot was performed on immunoprecipitated samples and cell lysates with primary antibody to HA (Covance MMS101R), Flag (Abcam, ab1162), PCNA (Abcam ab29), and CDKN1C (Santa Cruz biotechnology, sc-1040). Secondary antibodies used were goat-anti-mouse-HRP (Biorad, 1:20,000) and goat-anti-rabbit-HRP (Santa Cruz, 1:5,000).

Drosophila experiments

Five independent constructs, $CDKN1C^{WT}$, $CDKN1C^{L42P}$, $CKDN1C^{826delT}$, $CDKN1C^{F276V}$, and $CDKN1C^{K278E}$ were injected into embryos and each construct generated multiple independent transgenic lines. Overexpression was achieved by using the GAL4-UAS system[17] and the following drivers: *Ubi-gal4* (ubiquitous expression), *ey-gal4* (eye-specific expression), *MS1096-gal4* (wing-specific expression), and sal^{PE}*-gal4* (wing pouch-specific expression). *MS1096-gal4* is expressed in the entire wing imaginal disc but at higher levels in the dorsal compartment. This higher level of expression in the dorsal compartment causes enhanced phenotypic effects in the dorsal versus the ventral side of the wing. sal^{PE}*-gal4* is specifically expressed in the pouch of the wing disc, which only gives rise to the wing proper. All UAS-*CDKN1C* constructs were larval lethal when expressed with *Ubi-gal4*, confirming their expression efficiency. At least two independent lines were used for each experiment and all yielded similar results. All eye images were taken on a Leica Z16 AP0 Camera. Wing IMAGEs were taken on Leica DFC 300 FX R2 Camera.

Flow Cytometry

Wild-type or mutant versions of *CDKN1C* were co-transfected with pCMV-GFP into serum starved HEK293T cells using Lipofectamine 2000 (Invitrogen). After 24 hours, cells were

grown in media containing 5% serum for 48-hours. Cells were resuspended in a hypotonic buffer with propidium iodide and GFP-positive events were analyzed on a Becton Dickinson FACScan Analytic Flow Cytometer. All experiments were performed in 2 biological replicates. Statistical significance was assessed using a 2-proportion z-test. Flow cytometry was performed in the UCLA Johansson Comprehensive Cancer Center (JCCC) and Center for AIDS Research Flow Cytometry Core Facility.

Analysis of nuclear/cytoplasmic distribution of GFP-fusion proteins

H295R cells were transfected using Lipofectamine 2000. After incubation for 24 hours, cells were fixed in 4% paraformaldehyde and IHC was performed using an anti-GFP antibody (Invitrogen), a FITC-labeled secondary antibody (Jackson Lab), and a mounting medium with DAPI (VectorLabs). Cells were imaged on an Olympus AX70 microscope.

M1 fibroblasts were transfected with 2ug/well of purified expression plasmid using the X-tremeGENE HP DNA transfection reagent (Roche). 24-hours after transfection, cells were fixed in 2% formaldehyde and analyzed using fluorescence microscopy. Fluorescent and bright-field images of randomly selected fields containing transfected M1 cells were saved electronically using a 'blind-code' file nomenclature. The distribution of GFP-fusion proteins in each transfected cell was annotated by an experienced observer (who was unaware of the blind code) as one of the following: (1) nuclear only, (2) nuclear and cytoplasmic, and (3) cytoplasmic only.

Supplementary Material

Refer to Web version on PubMed Central for supplementary material.

Acknowledgments

This work was funded by the Doris Duke Charitable Foundation and NICHD RO1HD068138. V.A.A. was supported by NIH 1 F31HD068136 training grant. Human embryonic material was provided by the Medical Research Council/Wellcome Trust-funded Developmental Biology Resource (www.hdbr.org) (MRC 0700089; The Wellcome Trust GR082557). J.C.A. was supported by a Wellcome Trust Senior Research Fellowship in Clinical Science (079666). We thank Rafael Matera (NIH) for kindly providing the pCI-neo-(HA)3-ubiquitin construct. We thank Edward R.B. McCabe for initial critical support of adrenal research for E.V. and for providing one IMAGE patient sample.

References

1. Vilain E, et al. IMAGe, a new clinical association of intrauterine growth retardation, metaphyseal dysplasia, adrenal hypoplasia congenita, and genital anomalies. J Clin Endocrinol Metab. 1999; 84:4335–4340. [PubMed: 10599684]
2. Bergada I, et al. Familial occurrence of the IMAGe association: additional clinical variants and a proposed mode of inheritance. J Clin Endocrinol Metab. 2005; 90:3186–3190. [PubMed: 15769992]
3. Lee MH, Reynisdottir I, Massague J. Cloning of p57KIP2, a cyclin-dependent kinase inhibitor with unique domain structure and tissue distribution. Genes Dev. 1995; 9:639–649. [PubMed: 7729683]
4. Romanelli V, et al. CDKN1C (p57(Kip2)) analysis in Beckwith-Wiedemann syndrome (BWS) patients: Genotype-phenotype correlations, novel mutations, and polymorphisms. Am J Med Genet A. 2010; 152A:1390–1397. [PubMed: 20503313]
5. Hutz JE, et al. IMAGe association and congenital adrenal hypoplasia: no disease-causing mutations found in the ACD gene. Mol Genet Metab. 2006; 88:66–70. [PubMed: 16504561]

6. Ko JM, Lee JH, Kim GH, Kim AR, Yoo HW. A case of a Korean newborn with IMAGe association presenting with hyperpigmented skin at birth. Eur J Pediatr. 2007; 166:879–880. [PubMed: 17120039]
7. Lienhardt A, Mas JC, Kalifa G, Chaussain JL, Tauber M. IMAGe association: additional clinical features and evidence for recessive autosomal inheritance. Horm Res. 2002; 57 (Suppl 2):71–78. [PubMed: 12065932]
8. Pedreira CC, Savarirayan R, Zacharin MR. IMAGe syndrome: a complex disorder affecting growth, adrenal and gonadal function, and skeletal development. J Pediatr. 2004; 144:274–277. [PubMed: 14760276]
9. Tan TY, et al. Two sisters with IMAGe syndrome: cytomegalic adrenal histopathology, support for autosomal recessive inheritance and literature review. Am J Med Genet A. 2006; 140
10. Amano N, et al. Radiological evolution in IMAGe association: a case report. Am J Med Genet A. 2008; 146A:2130–2133. [PubMed: 18627061]
11. Balasubramanian M, Sprigg A, Johnson DS. IMAGe syndrome: Case report with a previously unreported feature and review of published literature. Am J Med Genet A. 2010; 152A
12. Watanabe H, et al. Suppression of cell transformation by the cyclin-dependent kinase inhibitor p57KIP2 requires binding to proliferating cell nuclear antigen. Proc Natl Acad Sci U S A. 1998; 95:1392–1397. [PubMed: 9465025]
13. Goujon M, et al. A new bioinformatics analysis tools framework at EMBL-EBI. Nucleic Acids Res. 2010; 38:W695–699. [PubMed: 20439314]
14. Adzhubei IA, et al. A method and server for predicting damaging missense mutations. Nat Methods. 2010; 7:248–249. [PubMed: 20354512]
15. Diaz-Meyer N, et al. Silencing of CDKN1C (p57KIP2) is associated with hypomethylation at KvDMR1 in Beckwith-Wiedemann syndrome. Journal of medical genetics. 2003; 40:797–801. [PubMed: 14627666]
16. Shin JY, Fitzpatrick GV, Higgins MJ. Two distinct mechanisms of silencing by the KvDMR1 imprinting control region. Embo J. 2008; 27:168–178. [PubMed: 18079696]
17. Brand AH, Perrimon N. Targeted gene expression as a means of altering cell fates and generating dominant phenotypes. Development. 1993; 118:401–415. [PubMed: 8223268]
18. Wiedemann HR. The EMG-syndrome: exomphalos, macroglossia, gigantism disturbed carbohydrate metabolism. Z Kinderheilkd. 1969; 106:171–185. [PubMed: 5797233]
19. Beckwith JB. Macroglossia, omphalocele, adrenal cytomegaly, gigantism, and hyperplastic visceromegaly. Birth Defects Orig Art Ser. 1969; V(2):188–196.
20. Zhang P, et al. Altered cell differentiation and proliferation in mice lacking p57KIP2 indicates a role in Beckwith-Wiedemann syndrome. Nature. 1997; 387:151–158. [PubMed: 9144284]
21. Hatada I, et al. An imprinted gene p57KIP2 is mutated in Beckwith-Wiedemann syndrome. Nat Genet. 1996; 14:171–173. [PubMed: 8841187]
22. Bourcigaux N, et al. High expression of cyclin E and G1 CDK and loss of function of p57KIP2 are involved in proliferation of malignant sporadic adrenocortical tumors. J Clin Endocrinol Metab. 2000; 85:322–330. [PubMed: 10634406]
23. Havens CG, Walter JC. Mechanism of CRL4(Cdt2), a PCNA-dependent E3 ubiquitin ligase. Genes Dev. 2011; 25:1568–1582. [PubMed: 21828267]
24. Kirchmaier AL. Ub-family modifications at the replication fork: Regulating PCNA-interacting components. FEBS Lett. 2011; 585:2920–2928. [PubMed: 21846465]
25. Ye Y, Rape M. Building ubiquitin chains: E2 enzymes at work. Nat Rev Mol Cell Biol. 2009; 10:755–764. [PubMed: 19851334]
26. Mukhopadhyay D, Riezman H. Proteasome-independent functions of ubiquitin in endocytosis and signaling. Science. 2007; 315:201–205.10.1126/science.1127085 [PubMed: 17218518]
27. Li W, Ye Y. Polyubiquitin chains: functions, structures, and mechanisms. Cell Mol Life Sci. 2008; 65:2397–2406. [PubMed: 18438605]
28. Thrower JS, Hoffman L, Rechsteiner M, Pickart CM. Recognition of the polyubiquitin proteolytic signal. Embo J. 2000; 19:94–102.10.1093/emboj/19.1.94 [PubMed: 10619848]

29. Lee H, Jen JC, Cha YH, Nelson SF, Baloh RW. Phenotypic and genetic analysis of a large family with migraine-associated vertigo. Headache. 2008; 48:1460–1467. [PubMed: 18081823]
30. Lee H, et al. Improving the efficiency of genomic loci capture using oligonucleotide arrays for high throughput resequencing. BMC Genomics. 2009; 10:646. [PubMed: 20043857]
31. Homer N, Merriman B, Nelson SF. BFAST: an alignment tool for large scale genome resequencing. PLoS One. 2009; 4:e7767. [PubMed: 19907642]
32. Homer N, Merriman B, Nelson SF. Local alignment of two-base encoded DNA sequence. BMC Bioinformatics. 2009; 10:175. [PubMed: 19508732]
33. Li H, et al. The Sequence Alignment/Map format and SAMtools. Bioinformatics. 2009; 25:2078–2079. [PubMed: 19505943]
34. Clark MJ, et al. U87MG Decoded: The Genomic Sequence of a Cytogenetically Aberrant Human Cancer Cell Line. PloS Genetics. 2009; 6
35. O'Connor BD, Merriman B, Nelson SF. SeqWare Query Engine: storing and searching sequence data in the cloud. BMC Bioinformatics. 11(Suppl 12):S2. [PubMed: 21210981]
36. Matsuoka S, et al. p57KIP2, a structurally distinct member of the p21CIP1 Cdk inhibitor family, is a candidate tumor suppressor gene. Genes Dev. 1995; 9:650–662. [PubMed: 7729684]
37. Mattera R, Tsai YC, Weissman AM, Bonifacino JS. The Rab5 guanine nucleotide exchange factor Rabex-5 binds ubiquitin (Ub) and functions as a Ub ligase through an atypical Ub-interacting motif and a zinc finger domain. The Journal of biological chemistry. 2006; 281

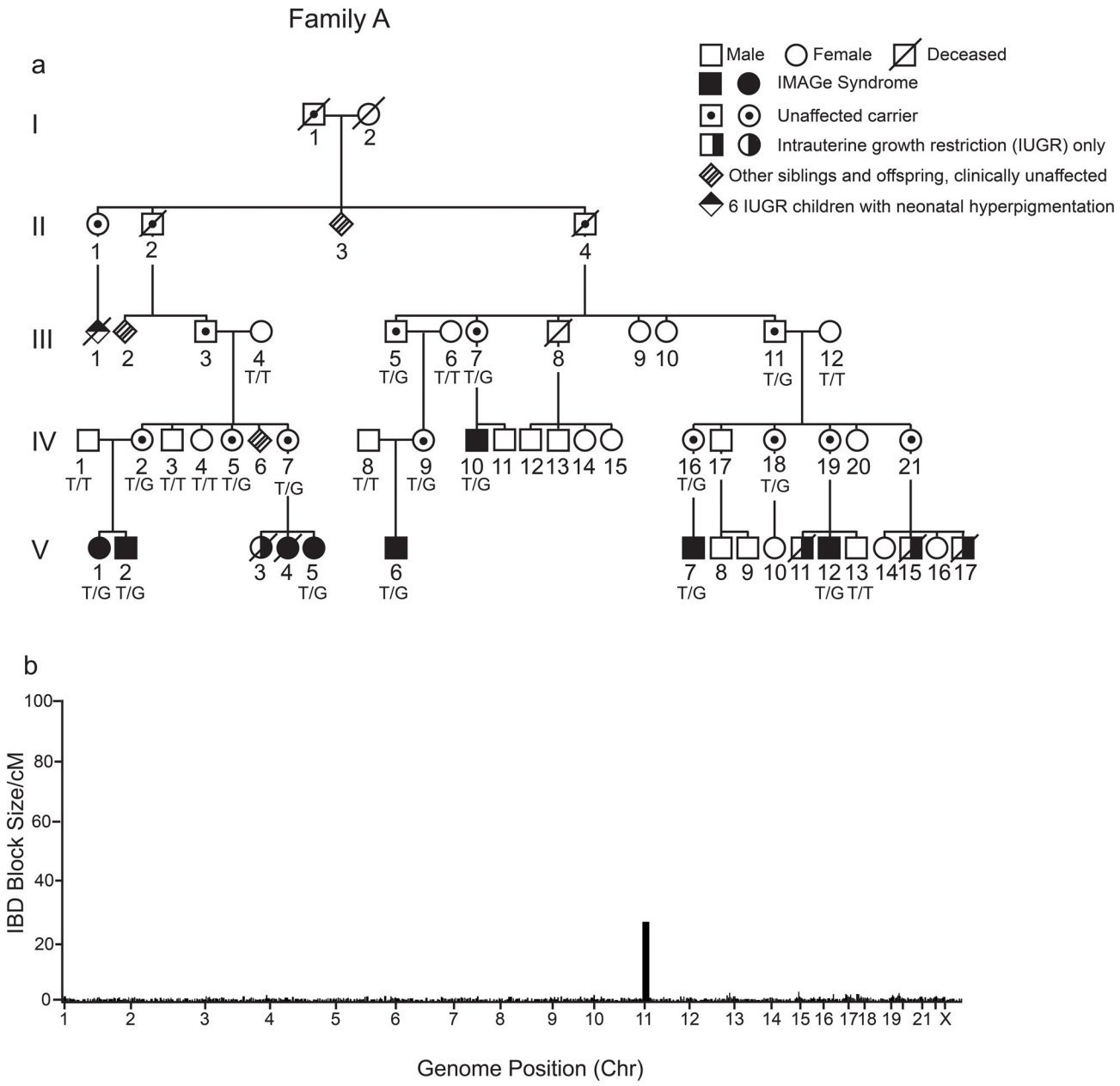

Figure 1. Identity-by-descent analysis in a family with IMAGE syndrome

(a) In this large family (Family A) with IMAGE syndrome[2], 24 individuals were tested for genetic mutations in *CDKN1C*. All affected individuals we tested carried the c.825T>G mutation on the maternally inherited allele resulting in a F276V amino acid change. Unaffected carriers all inherited the mutations on the paternal alleles. (b) IBD analysis identified a region on chromosome 11 spanning from base pairs 2,685,916 to 19,809,755 (according to hg19) that was shared by affected family members (IV-10, V-1, V-2, V-5, V-6, V-7, V-12) and different from an unaffected sibling (V-13).

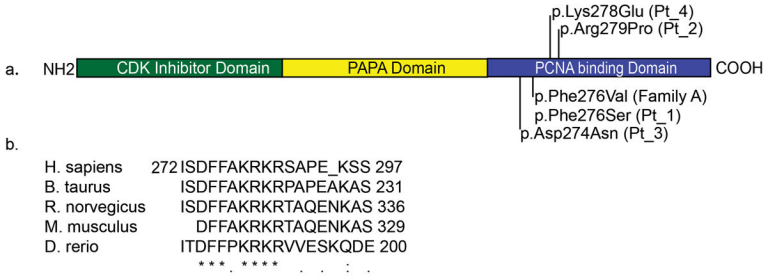

Figure 2. Localization of IMAGE syndrome mutations in *CDKN1C*

(a) All IMAGE syndrome mutations are localized to the region of the gene encoding the PCNA-binding domain. (b) Highly conserved amino acid residues (indicated by *) in the PCNA-binding domain of *CDKN1C* are conserved down to *D. rerio*. All IMAGE mutations affect highly conserved residues. A colon (:), indicates conservation between groups of strongly similar properties; a period indicates conservation between groups of weakly similar properties.

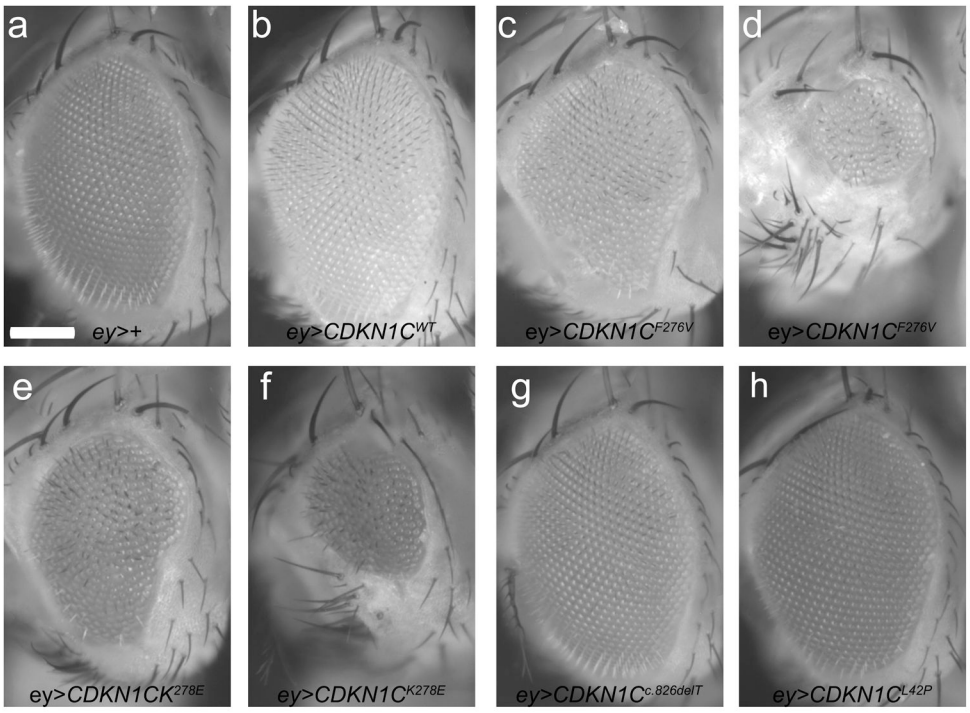

Figure 3. Phenotypic validation of IMAGE syndrome-associated mutations in *Drosophila melanogaster*

(**a**) Light microscope IMAGE of an adult wild type eye (*ey>+*). Scale bar, 25μm. (**b**) Eye-specific expression of human *CDKN1C* (*ey>CDKN1C* ^{WT}) did not affect final size. (**c-g**) Overexpression of IMAGE syndrome-associated human *CDKN1C* mutations F276V (**c-d,** *ey>CDKN1C*^{F276V}) or K278E (**e-f,** *ey>CDKN1C*^{K278E}) in the developing eye led to a gain-of-function phenotype of moderate (**c**, **e**) to severely (**d**, **f**) restricted eye growth. (**g-h**) Overexpression of human *CDKN1C* carrying Beckwith-Wiedemann syndrome-associated mutations, c.826delT (**g,** *ey>CDKN1C*^{826delT}) or L42P (**h,** *ey>CDKN1C*^{L42P}), did not affect eye growth.

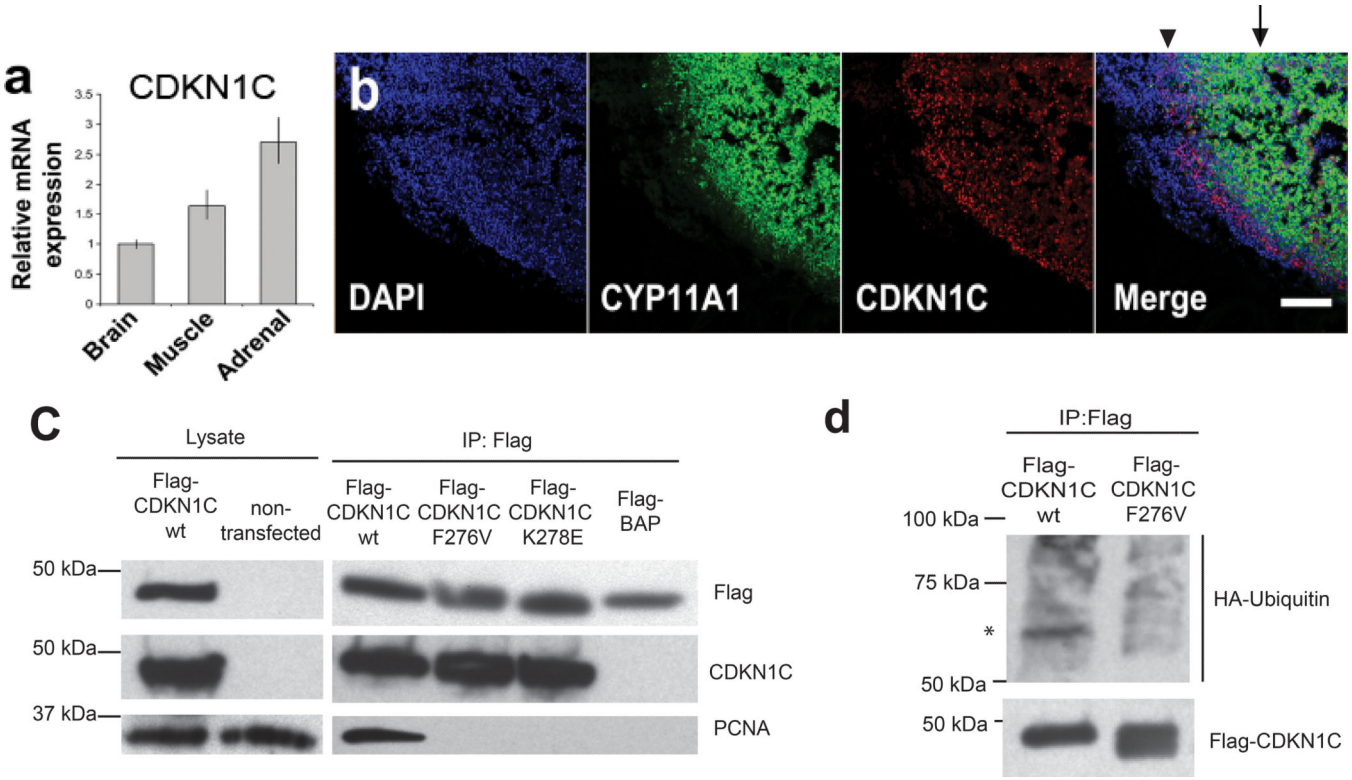

Figure 4. *CDKN1C* is expressed in the developing human adrenal gland and IMAGE mutants lose PCNA-binding, altering ubiquitination of CDKN1C

(a) Taqman RT-PCR showed higher expression of *CDKN1C* in the adrenal gland at 7–8 weeks post conception compared to control samples (muscle, brain). Error bars represent 1 s.d. (b) Immunohistochemistry showed *CDKN1C* protein expression in the developing adrenal gland at 8 weeks post conception. Nuclear expression of *CDKN1C* was observed in a subset of cells in the subcapsular region (arrowhead) and developing definitive cortex (arrow). Expression of the steroidogenic enzyme CYP11A1 is shown, predominantly in the fetal zone of the developing gland. Nuclear counterstaining was performed with DAPI. Scale bar, 200 μm. (c) HEK293T cells transfected with flag-tagged wild type or IMAGE mutant (F276V or K278E) CDKN1C were immunoprecipitated with Flag antibody. Left panel: whole lysates for wild type and non-transfected cells. Right panel: Flag immunoprecipitated fraction binds with endogenous PCNA in wild type but not in IMAGE mutants F276V and K278E. Flag-BAP: Bacterial Alkaline Phosphatase. (d) Immunoprecipitation of HEK293T cells co-transfected with Flag-CDKN1C (wild type or F276V) and HA-Ubiquitin constructs. Top panel: Immunoblot with HA antibody identifies a band at ~63kDa (indicated by *) in the CDKN1C wild type that is not present in the F276V IMAGE mutant. Bottom panel: Immunoblot of Flag protein.

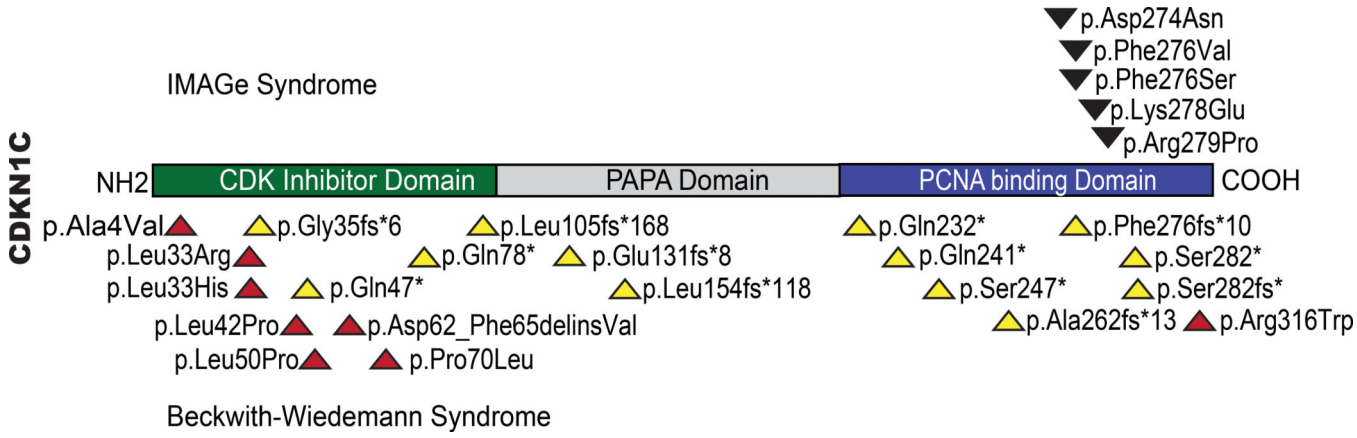

Figure 5. Missense mutations in CDK-binding domain and truncating mutations in CDKN1C cause Beckwith-Wiedemann Syndrome while missense mutations localized to the PCNA-binding domain result in IMAGE syndrome

Comparison between *CDKN1C* mutations resulting in IMAGE Syndrome (black arrowheads located above gene) or in Beckwith-Wiedemann Syndrome (below; red arrowheads = missense mutations; yellow arrowheads = truncating mutations). BWS mutations are either missense mutations primarily located in the cyclin-binding domain or truncating mutations, while IMAGE syndrome mutations are all missense mutations localized to a highly conserved region of the PCNA-binding domain.

Table 1

Clinical characteristics of IMAGE Syndrome Patients

	Pt 1	Pt 2	Pt 3	Pt 4	IV-10	V-12	V-7	V-6	V-5	V-1	V-2
Chromosomal sex	46, XY	46, XY	46, XY	46,XY	46, XY	46, XY	46, XY	46, XY	46, XX	46, XX	46, XY
Nucleotide Change	826T>C	835G>C	819G>A	831A>G	825T>G	825T>G	825T>G	825T>G	825T>G	825T>G	825T>G
Amino Acid Change	Phe276Ser	Arg279Pro	Asp274Asn	Lys278Glu	Phe276Val	Phe276Val	Phe276Val	Phe276Val	Phe276Val	Phe276Val	Phe276Val
Intrauterine Growth Restriction	+	+	+	+	+	+	+	+	+	+	+
Adrenal crisis	+ (day 14)	+ (day 4)	+ (day 7)	+ (day 3)	+ (day 11)	+ (1st week)	+ (day11)	+ (day19)	+ (day20)	+ (day5)	+ (day21)
Adrenal hypoplasia	probable	+	+	+	+	+	+	+	+	+	+
Hypercalciuria	+	+	probable	+	NE	NE	NE	NE	−	NE	NE
Bifrontal bossing, abnormal ears and nose	+	+	+	+	+	+	+	+	+	+	+
Short arms and legs	+	+	+	+	−	−	−	−	+	−	−
Craniosynostosis	+	+	+	−	−	−	−	−	−	−	−
Genital Anomalies	+	+	small penis	+	+	+	+	−	NA	NA	−
Cryptorchidism Unilateral or bilateral	+	+	+	+	+	−	−	+	NA	NA	+
Osteopenia	+	+	+	NE	NE	NE	NE	NE	NE	NE	NE
Delayed bone age	+	+	+	+	+	+	+	+	+	−	+
Small epiphyses	+	−	+	+	+	+	−	+	NE	−	+
Striated irregular metaphyses	+	+	+	+*	+	+	−	+	NE	−	+

NE: Not Evaluated; NA: Not Applicable; day refers to the postnatal day of adrenal crisis.

* broad and flattened, but not striated